

# High growth-rate atomic layer deposition process of cerium oxide thin film for solid oxide fuel cell

Jin-Geun Yu<sup>a,1</sup>, Byung Chan Yang<sup>a,1</sup>, Jeong Woo Shin<sup>a</sup>, Sungje Lee<sup>a</sup>, Seongkook Oh<sup>a</sup>,  
Jae-Ho Choi<sup>b</sup>, Jaehack Jeong<sup>b</sup>, Wontae Noh<sup>c</sup>, Jihwan An<sup>a,\*</sup>

<sup>a</sup> Department of Manufacturing Systems and Design Engineering (MSDE), Seoul National University of Science and Technology (SeoulTech), 232 Gongneung-ro, Nowon-gu, Seoul 01811, Republic of Korea

<sup>b</sup> CN1 Co., Ltd., Dongtansandan 7-gil, Dongtan-myeon, Hwaseong-si, Gyeonggi-do, Republic of Korea

<sup>c</sup> Air Liquide Laboratories Korea, Yonsei-ro 50, Seodaemun-gu, Seoul, Republic of Korea

## ARTICLE INFO

### Keywords:

Atomic layer deposition  
Cerium oxide  
Solid oxide fuel cell  
Interlayer  
Thermal stability

## ABSTRACT

Cerium oxide (CeO<sub>2</sub>) shows superior surface exchange, and therefore is widely used for the cathode interlayer coating material to reduce the activation loss in low temperature solid oxide fuel cell (LT-SOFC). Here, we report on the application of the high growth-rate atomic layer deposition (ALD) process of CeO<sub>2</sub> thin films as cathodic interlayers for LT-SOFCs. We demonstrate that the maximum power density of the SOFC with pure CeO<sub>2</sub> interlayer increases by 45% compared to the one without interlayer at 450 °C. More importantly, the performance degradation rate of the ALD CeO<sub>2</sub> interlayered cell improves by 25 times compared to the cell without interlayer during 24 h operation at 450 °C.

## 1. Introduction

Solid oxide fuel cells (SOFCs) are drawing lots of attention as next-generation energy conversion devices due to their advantages such as high energy conversion efficiency, fuel flexibility, and environmental friendliness [1,2]. In case of conventional SOFCs, high operating temperature of 800–1000 °C should be usually maintained, which often causes problems in durability and applicability to wider range of applications. Therefore, research on low temperature (operating temperature < 500 °C) solid oxide fuel cell (LT-SOFC) is needed to lower the operating temperature while maintaining a reasonably high power density [3]. Reducing the activation loss at cathode is especially essential in acquiring high performance LT-SOFC due to sluggish oxygen reduction reaction (ORR) at cathode [4–7]. The increase of activation loss for ORR is indeed the main cause of the decrease of maximum power density of LT-SOFC [8].

CeO<sub>2</sub>-based materials are widely used for LT-SOFCs because they generally have higher oxygen ion conductivity and oxygen surface exchange coefficient than widely used ZrO<sub>2</sub>-based materials [9]. When used as interlayers between cathode and electrolyte, CeO<sub>2</sub>-based material can significantly enhance the surface oxygen exchange and therefore lower the cathodic activation loss [10]. Among various techniques to deposit CeO<sub>2</sub> layer, atomic layer deposition (ALD) is

interesting because the thickness of the thin film can be controlled in sub-nm level, uniform thin film can be grown compared to other vapor deposition methods, and it is possible to deposit conformal films on a complex structure. These advantages stem from a self-limiting nature of ALD process [11]. It has been reported that when only 10 nm-thick ALD yttria-doped ceria (YDC) is used as an interlayer, a maximum power density of the SOFC increased by a factor of 2 [12]. Usually much thicker (> 50–100 nm) films are known to be needed for similar effects when the interlayer is processed by physical vapor deposition (PVD) methods such as PLD or sputtering [13,14]. Nevertheless, the ALD CeO<sub>2</sub> process shown in the previous literature used the β-diketonate type Ce precursor (Ce(thd)<sub>4</sub> (thd = 2,2,6,6-tetramethyl-3,5-heptanedionate)), whose use may be limited due to extremely slow growth-rate per cycle (GPC, < 0.1 nm/cycle) and low volatility.

In this paper, we deposit the ALD CeO<sub>2</sub> thin film using cyclopentadienyl type ((i-PrCp)<sub>3</sub>Ce, (tris(isopropylcyclopentadienyl) cerium)) precursor, which has high vapor pressure and high GPC (> 0.3 nm/cycle), and apply it as the cathode interlayer of LT-SOFC. Not only the improvement (45%) in the maximum power density, as was reported many times previously, but also the significant enhancement in thermal stability, i.e., performance degradation decreased to 1.5%/h from 40%/h (reference) was observed.

\* Corresponding author.

E-mail address: [jihwanan@seoultech.ac.kr](mailto:jihwanan@seoultech.ac.kr) (J. An).

<sup>1</sup> These authors contributed equally to this work.

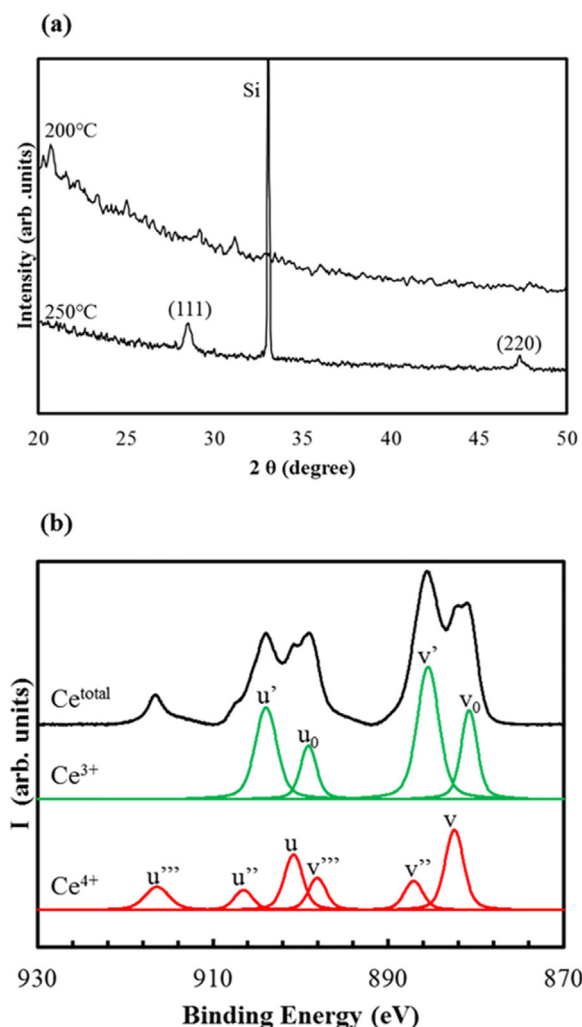


Fig. 1. (a) XRD spectra of ALD  $\text{CeO}_2$  films deposited at 200 and 250 °C on Si wafer and (b) high resolution XPS spectra near Ce 3d peaks with  $\text{Ce}^{3+}$  and  $\text{Ce}^{4+}$  reference peaks.

## 2. Experimental

For the ALD  $\text{CeO}_2$  process, tris(isopropyl-cyclopentadienyl) cerium ( $(i\text{-PrCp})_3\text{Ce}$ ) (Air Liquide Korea, 99%-Ce) and distilled water (Daejung Chemical, HPLC) were used as Ce precursor and oxidant, respectively. A house-built ALD station was used for the deposition [7]. The temperature of cerium precursor canister was fixed at 150 °C and the water at room temperature. Nitrogen gas was used as a carrier gas with a flow rate of 20 sccm. One cycle of ALD process consists of (1) injection of a 0.5 s cerium precursor (2) 30 s cerium precursor removal, (3) 0.1 s oxidant injection, and (4) 30 s oxidant removal steps. The growth rate per cycle was measured to be  $\sim 0.3$  nm/cycle at 200 °C.

To make a fuel cell, a yttria-stabilized zirconia (YSZ) substrate (300  $\mu\text{m}$  thick, polycrystalline, 1 cm  $\times$  1 cm, one side polished, MTI Korea) was used as electrolyte. For the reference cell, both sides (cathode and anode) of the YSZ substrate was deposited with 80 nm porous Pt using DC-sputtering at a DC power of 300 W and a Ar pressure of 40 mTorr [7]. For the cell with an interlayer, one side (cathode side) of the YSZ substrate was coated with ALD  $\text{CeO}_2$  thin film (70 cycles,  $\sim 23$  nm-thick) at the deposition temperature of 200 °C (Fig. S1), and then porous Pt electrodes were deposited on both sides.

Atomic force microscope (AFM) (Veeco, diDimension™ 3100) was used for morphological analysis. X-ray diffraction (XRD) (Bruker, DE/D8 Advance) was used to analyze the crystallinity of the films. X-ray

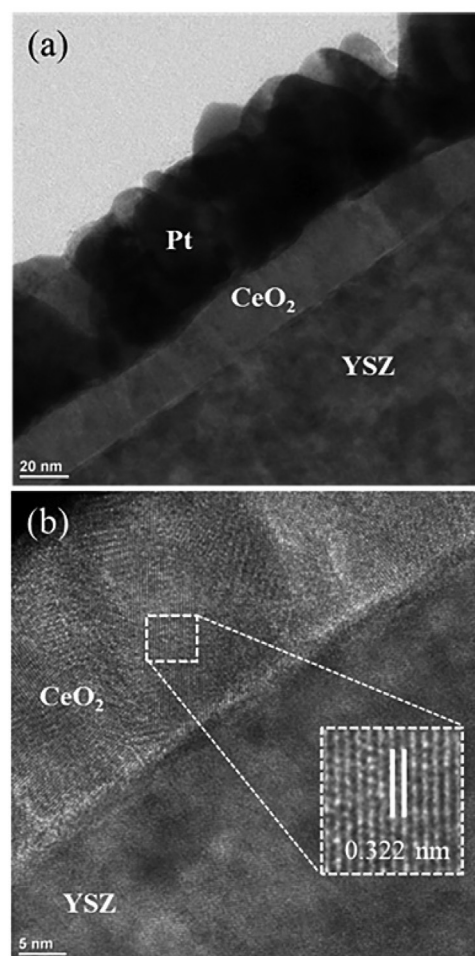


Fig. 2. (a) Cross-sectional TEM image of the cell with interlayer after operation for 24 h at 450 °C: Pt cathode/ $\text{CeO}_2$  interlayer/YSZ substrate are shown. (b) Zoomed-in image near  $\text{CeO}_2$ -YSZ interface.

photoelectron spectroscopy (XPS) (ThermoFisher Scientific, K-Alpha+) was used to analyze the chemical composition with an Al  $K\alpha$  source gun, a spot size of 400  $\text{nm}^2$  and a binding energy range of 0–1000 eV. To observe the cross-sectional morphology, a transmission electron microscope (TEM, FEI Tecnai F30 S-TWIN) was used at the acceleration voltage of 300 kV.

Electrochemical performances of the SOFC samples were analyzed in a customized test station built on a temperature-controllable heater [7]. Dry hydrogen gas (20 sccm) was flown to the anode, and the ambient air to the cathode. Electrochemical analysis was performed at 450 °C using a potentiostat (Sp-200, Bio-logic). Electrochemical impedance spectroscopy (EIS) analysis was conducted in the frequency range of 1 MHz to 1 Hz with a sinusoidal AC voltage of 50 mV in amplitude at cell voltages of open circuit voltage (OCV) and 0.6 V. For durability analysis, electrochemical analysis was performed at 450 °C for 24 consecutive hours.

## 3. Result and discussion

In the AFM image of ALD  $\text{CeO}_2$  film on Si wafer, the film shows polycrystalline nature with nanoscale grains of the average grain size of  $18.9 \pm 5.0$  nm (Fig. S2). The root mean square (RMS) surface roughness is only 0.9 nm, which confirms a very smooth surface. Such small grains render the high density of surface grain boundaries, where oxygen exchange and oxygen absorption tend to occur more actively than at the center of the grain [15,16]. XRD analysis shows that the crystallization of ALD  $\text{CeO}_2$  thin films improves, or grain size becomes

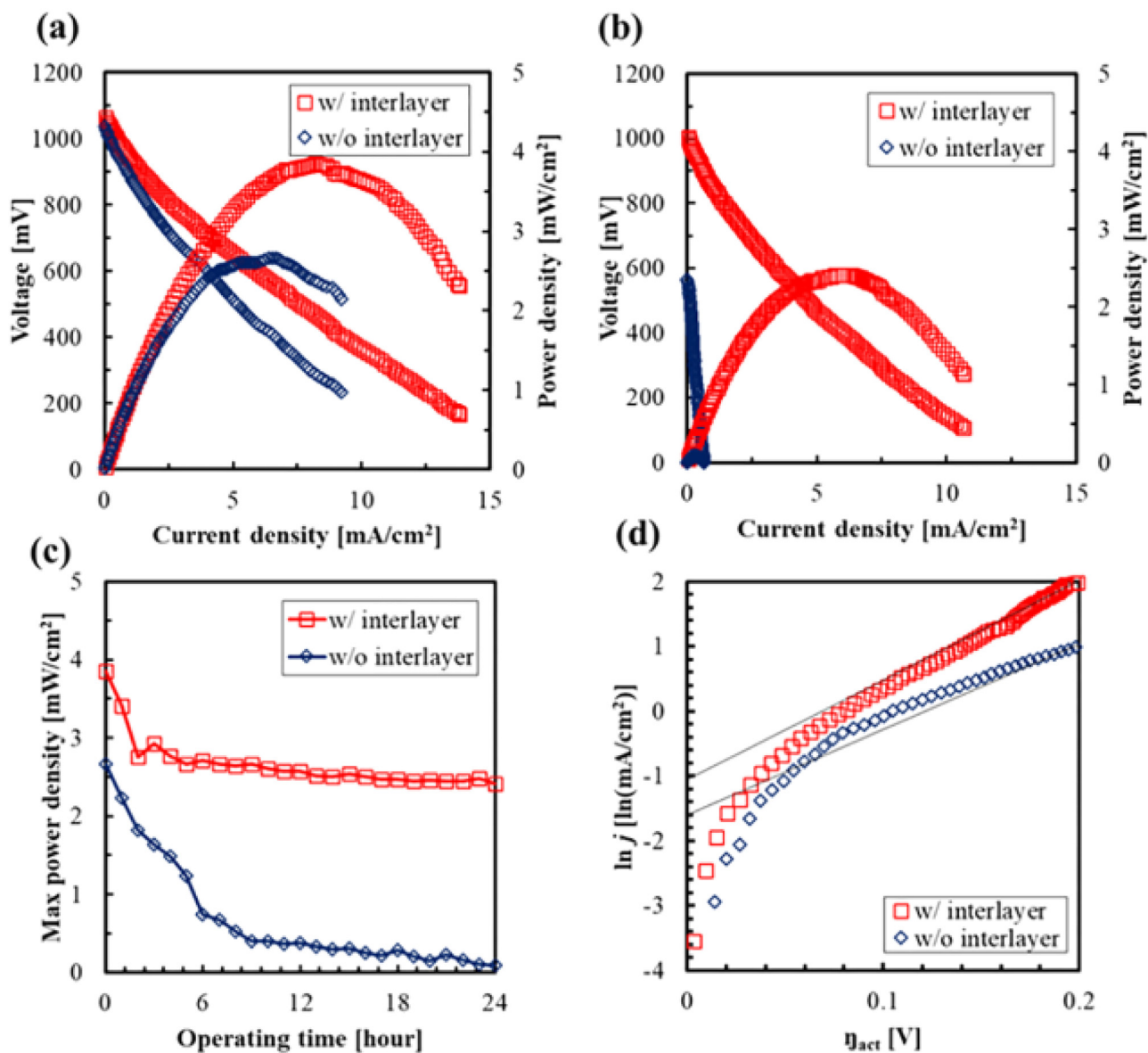


Fig. 3. I-V-P curves of SOFCs with interlayer and the one without interlayer (a) after 0 h and (b) after 24 h of operation at 450 °C. (c) Maximum power density changes of the cells during 24 h. (d) Tafel plot of the cells with and without interlayers at 450 °C at 0 h.

larger, when the deposition temperature increases from 200 °C to 250 °C even in the as-deposited films without the use of plasma. (Fig. 1(a)) [17]. In the previous paper, better crystallinity or larger grain size of interlayer thin film was shown to be less beneficial in activation process compared to that with smaller grains [16]. Therefore, the film deposited at 200 °C was adopted as the interlayer for further analysis.

XPS analysis showed that the composition of Ce is 33.9%, O is 63.0 at%, and C is 3.1 at% in the CeO<sub>2</sub> film (Fig. S3). The carbon content may have stem from the partially incomplete ligand exchange reaction between the Ce precursor and the oxidant. The high resolution scan near Ce 3d peaks further reveals the relative composition of Ce with different valence states (Fig. 1(b)). In case of CeO<sub>2</sub>, the composition of Ce<sup>3+</sup> and Ce<sup>4+</sup> can vary depending on the deposition environment, e.g., oxidant partial pressure, temperature, etc [18]. We can use the v peaks to find the ratio between Ce<sup>3+</sup> and Ce<sup>4+</sup>, and the concentration of Ce<sup>3+</sup> can be calculated using following equation was calculated to be 62% with the rest (38%) corresponding to Ce<sup>4+</sup> out of total Ce content. The relatively high Ce<sup>3+</sup> content could be due to the low partial pressure (~1 Torr) of the oxidant (water) in the ALD

oxidation step.

TEM images (Fig. 2(a) and (b)) show the Pt/CeO<sub>2</sub>/YSZ interface at the cathode of the LT-SOFC after operation for 24 h at 450 °C. Sharp and dense interface without any physical pores is observed, and the thickness of ALD CeO<sub>2</sub> layer is confirmed to be ~23 nm. The lattice spacing shown in the inset image in Fig. 3(b) is 0.322 nm, which corresponds to (111) crystallographic plane in cubic CeO<sub>2</sub>. Also the lattice parameter calculated based on this measurement is 0.557 nm. While the lattice parameter of cubic stoichiometric CeO<sub>2</sub> has been reported to be 0.541 nm, it tends to increase as more oxygen is deficient, i.e., x in CeO<sub>x</sub> decreases. It has been reported the lattice parameter of cerium oxide can be as large as 0.557 nm as x in CeO<sub>x</sub> becomes ~1.7, which agrees well with our observation. Large concentration of Ce<sup>3+</sup> in XPS analysis (Fig. 1(b)) of our sample implies that the oxygen deficiency in our ALD CeO<sub>2</sub> film may have expanded the lattice.

The current–voltage–power (I–V–P) curves of the cells with and without ALD CeO<sub>2</sub> interlayers after 0 h and 24 h operation at 450 °C are shown in Fig. 3(a) and (b). Several points are to be made here: first, both the cells with interlayer and without interlayer show OCVs in the range of 1.03–1.05 V, which approximates to the theoretical OCV value

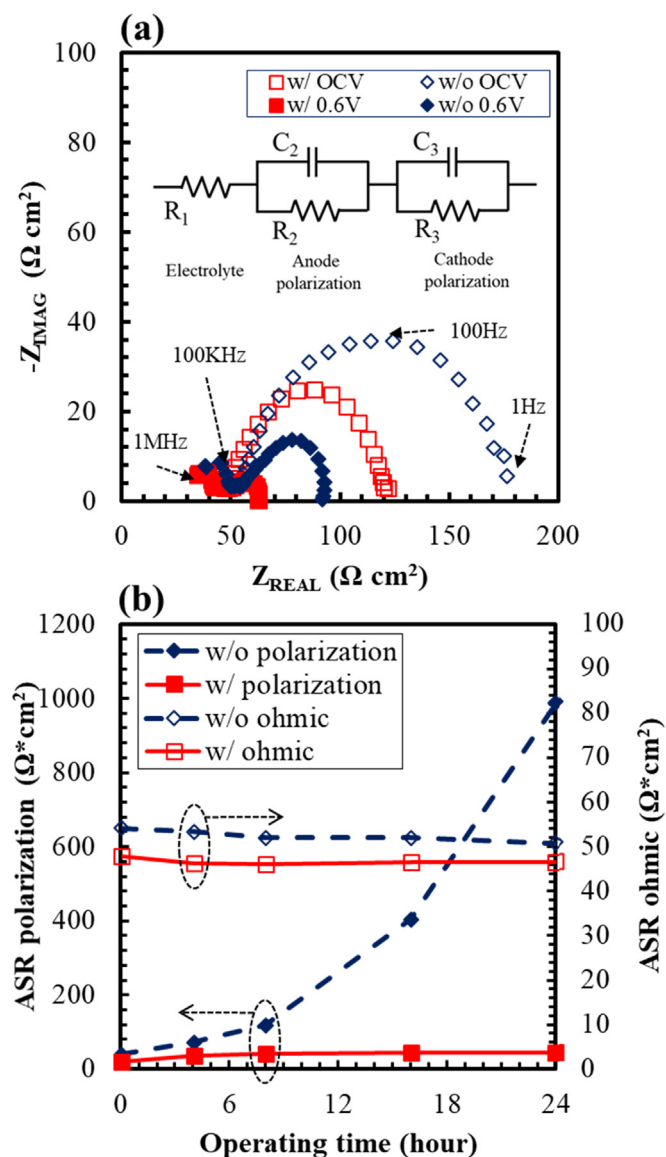


Fig. 4. (a) EIS spectra of SOFCs with and without interlayers at 450 °C at OCV and 0.6 V and the equivalent circuit model. (b) Summary of ohmic and polarization resistances of SOFCs with and without interlayers at 450 °C at 0.6 V during 24 h operation.

of 1.1 V when H<sub>2</sub> gas is used as fuel at 450 °C. The maximum power density of the cell without CeO<sub>2</sub> interlayer at 450 °C showed an initial maximum power density of 2.66 mW/cm<sup>2</sup>. On the other hand, the cell with CeO<sub>2</sub> interlayer had an initial maximum power density of 3.85 mW/cm<sup>2</sup> at 450 °C, showing the improvement by about 45% compared to the one without interlayer. This is due to intrinsically higher surface reaction rate at Pt-CeO<sub>2</sub> interface than at Pt-YSZ interface as well as higher surface grain boundary density. Tafel plot can be further used to observe the difference in surface oxygen exchange rate between the CeO<sub>2</sub> surface and the YSZ surface (Fig. 3(d)). The activation overvoltage ( $\eta_{act}$ ) of the fuel cell, which is the x axis of the Tafel plot, is calculated as follows [5].

$$\eta_{act} = OCV - V_{meas} - \eta_{ohmic} = OCV - V_{meas} - j \cdot ASR_e$$

( $\eta_{act}$ : activation loss, OCV: open circuit voltage,  $V_{meas}$ : the measured cell voltage,  $\eta_{ohmic}$ : ohmic overvoltage (loss),  $j$ : the current density,  $ASR_e$ : the area specific resistance of the electrolyte)

The exchange current density of the cell with CeO<sub>2</sub> interlayer extracted from the Tafel plot (y intercept of the fitting line when

$\eta_{act} > \sim 0.1$  V in Tafel plots [8]) is 0.37 mA/cm<sup>2</sup> at 450 °C, which is slightly lower than that at doped CeO<sub>2</sub> (YDC) surface (0.48 mA/cm<sup>2</sup>) reported elsewhere [5]. However, this value is still 75% higher than that of the cell without interlayer (0.21 mA/cm<sup>2</sup>) at YSZ-Pt interface.

Also note that the CeO<sub>2</sub> interlayer affect not only the initial performance but also the thermal stability of the cell (Fig. 3(c)). When continuously operated for 24 h, the cell with interlayer still shows a relatively high maximum power density of 2.42 mW/cm<sup>2</sup>, while the cell without interlayer shows negligible performance (0.1 mW/cm<sup>2</sup>) with significantly reduced OCV ( $\sim 0.6$  V) (Fig. 3(b)). In terms of the average performance degradation rate, the cell with and without interlayer showed 1.5%/h and 40%/h, respectively.

EIS analysis was performed to investigate the contribution of individual processes to the performance in the fuel cell operation and the change of the resistances associated with the processes. In general, the EIS can measure the magnitude of the ohmic resistance associated with ionic transport in electrolyte that does not change depending on the cell voltage (shown in high frequency region), and the polarization resistance associated with electrodes that change along the cell voltage (shown in low frequency region) (Fig. 4(a)) [5]. When Pt is used as catalytic electrode both for cathode and for anode, the polarization resistance generated at anode is very small compared to that at cathode, and therefore the size of the polarization resistance in the EIS spectra can be regarded to be coming from cathode. The polarization resistance of the cell with interlayer is over 50% less than that without interlayer at OCV and at 0.6 V (Fig. 4(a)). The decrease in the polarization resistance means that the activation loss for the ORR is reduced because the surface oxygen exchange reaction occurs cell on the surface of CeO<sub>2</sub> than on the surface of YSZ [7]. In addition, it is clearly shown that the change in the maximum power density over time is due to the change in the activation loss (Fig. 4(b)). The ohmic resistance of the cells are constant over time at 45–50  $\Omega \text{ cm}^2$ . In contrast, the polarization resistance of the cell without interlayer dramatically increases by  $\sim 25$  times (40  $\rightarrow$  986  $\Omega \text{ cm}^2$ ) over 24 h, while the increase of the polarization resistance of the cell without interlayer is only by 30% (19  $\rightarrow$  24  $\Omega \text{ cm}^2$ ).

Initial performance enhancement by inserting ALD CeO<sub>2</sub> interlayer seems to be due to two reasons: structural and material aspects. From the structural point of view, the nanocrystalline nature of ALD CeO<sub>2</sub> film that is due to relatively low deposition temperature (200 °C) is beneficial for expediting surface reaction, because large density of catalytically-active (i.e., smaller activation energy for oxygen incorporation) grain boundaries are exposed at surface. For instance, based on the brick layer model, the density of surface grain boundary of our ALD CeO<sub>2</sub> film (average grain size  $\sim 19$  nm) will be  $\sim 2$  orders of magnitude larger than that of polycrystalline material with microscale grain size. From the material point of view, the exchange current density at CeO<sub>2</sub>-Pt interface is known to be several orders of magnitude higher than that at YSZ-Pt interface, which can be even higher if CeO<sub>2</sub> is doped [5]. Combined effect in these two aspects may have contributed to the low activation resistance that led to the high performance.

It is also notable that performance degradation in the ALD CeO<sub>2</sub> interlayered cell is mitigated. High surface grain boundary density may have also contributed in this improvement; there is a report that the bond strength between the oxide support and the metal cluster is stronger at the grain boundary compared to the grain center [19]. In addition, the study on the bonding strength between Pt and different metal oxides has shown that the bond strength between CeO<sub>2</sub> and Pt is stronger than that between YSZ and Pt [20,21]. Such strong bonding may have impeded the migration of Pt clusters on ALD CeO<sub>2</sub> surface, which has resulted in the increased durability of LT-SOFC. More in-depth investigation is on-going in these aspects.

#### 4. Conclusion

We have deposited and characterized the ALD CeO<sub>2</sub> thin film

(~23 nm) with highly volatile Ce precursor ((i-PrCp)<sub>3</sub>Ce) that shows high GPC (> 0.3 nm/cycle). We have shown that the ALD CeO<sub>2</sub> has very fine nano-granular (~20 nm in grain size) structure with significant Ce<sup>3+</sup> content (~60% out of total Ce content). We further employed the ALD CeO<sub>2</sub> thin film as the cathode interlayer of LT-SOFC, and demonstrated that the maximum power density increases by 45%, the exchange current density increases by 75%, and also the performance degradation rate is reduced by 25 times compared to the one without interlayer at 450 °C. We think that the highly reactive and thermally stable metal catalyst-CeO<sub>2</sub> interface reported in this study may have implications in designing high performance energy conversion devices.

## Acknowledgements

This study was supported by the Research Program funded by the SeoulTech (Seoul National University of Science and Technology) (2017-1006). Authors thank Air Liquide Laboratories Korea for providing Ce precursor.

## Appendix A. Supporting information

Supplementary data associated with this article can be found in the online version at [doi:10.1016/j.ceramint.2018.11.050](https://doi.org/10.1016/j.ceramint.2018.11.050).

## References

- [1] M. Dokiya, SOFC system and technology, *Solid State Ion.* 152–153 (2002) 383–392, [https://doi.org/10.1016/S0167-2738\(02\)00345-4](https://doi.org/10.1016/S0167-2738(02)00345-4).
- [2] S.C. Singhal, Solid oxide fuel cells for stationary, mobile, and military applications, *Solid State Ion.* 152–153 (2002) 405–410, [https://doi.org/10.1016/S0167-2738\(02\)00349-1](https://doi.org/10.1016/S0167-2738(02)00349-1).
- [3] D.J.L. Brett, A. Atkinson, N.P. Brandon, S.J. Skinner, Intermediate temperature solid oxide fuel cells, *Chem. Soc. Rev.* 37 (2008) 1568, <https://doi.org/10.1039/b612060c>.
- [4] S. Ji, G.Y. Cho, W. Yu, P.C. Su, M.H. Lee, S.W. Cha, Plasma-enhanced atomic layer deposition of nanoscale yttria-stabilized zirconia electrolyte for solid oxide fuel cells with porous substrate, *ACS Appl. Mater. Interfaces* 7 (2015) 2998–3002, <https://doi.org/10.1021/am508710s>.
- [5] J. An, Y.B. Kim, J. Park, T.M. Gür, F.B. Prinz, Three-dimensional nanostructured bilayer solid oxide fuel cell with 1.3 W/cm<sup>2</sup> at 450C, *Nano Lett.* 13 (2013) 4551–4555, <https://doi.org/10.1021/nl402661p>.
- [6] Z. Fan, F.B. Prinz, Enhancing oxide ion incorporation kinetics by nanoscale Yttria-doped ceria interlayers, *Nano Lett.* 11 (2011) 2202–2205, <https://doi.org/10.1021/nl104417n>.
- [7] S. Oh, J. Park, J.W. Shin, B.C. Yang, J. Zhang, D.Y. Jang, J. An, High performance low-temperature solid oxide fuel cells with atomic layer deposited-yttria stabilized zirconia embedded thin film electrolyte, *J. Mater. Chem. A* 6 (2018) 7401–7408, <https://doi.org/10.1039/c7ta10678e>.
- [8] R. O'hayre, S.-W. Cha, W. Colella, F.B. Prinz, *Fuel cell fundamentals*, 3rd Ed., John Wiley & Sons, Honoken, 2016.
- [9] Y. Lee, Y. Choa, Synthesis and characterization of a ceria based composite electrolyte for solid oxide fuel cells by an ultrasonic spray pyrolysis process, *J. Kor. Powd. Met. Inst.* 21 (2014) 222–228, <https://doi.org/10.4150/KPMI.2014.21.3.222>.
- [10] J. Bae, S. Hong, B. Koo, J. An, F.B. Prinz, Y.B. Kim, Influence of the grain size of samaria-doped ceria cathodic interlayer for enhanced surface oxygen kinetics of low-temperature solid oxide fuel cell, *J. Eur. Ceram. Soc.* 34 (2014) 3763–3768, <https://doi.org/10.1016/j.jeurceramsoc.2014.05.028>.
- [11] T. Suntola, Atomic layer epitaxy, *Mater. Sci. Rep.* 4 (1989) 261–312, [https://doi.org/10.1016/S0920-2307\(89\)80006-4](https://doi.org/10.1016/S0920-2307(89)80006-4).
- [12] Z. Fan, J. An, A. Iancu, F.B. Prinz, Thickness effects of yttria-doped ceria interlayers on solid oxide fuel cells, *J. Power Sources* 218 (2012) 187–191, <https://doi.org/10.1016/j.jpowsour.2012.06.103>.
- [13] Y.B. Kim, T.P. Holme, T.M. Gür, F.B. Prinz, Surface-modified low-temperature solid oxide fuel cell, *Adv. Funct. Mater.* 21 (2011) 4684–4690, <https://doi.org/10.1002/adfm.201101058>.
- [14] T. Park, Y.H. Lee, G.Y. Cho, S. Ji, J. Park, I. Chang, S.W. Cha, Effect of the thickness of sputtered gadolinia-doped ceria as a cathodic interlayer in solid oxide fuel cells, *Thin Solid Films* 584 (2015) 120–124, <https://doi.org/10.1016/j.tsf.2015.03.010>.
- [15] J.H. Shim, J.S. Park, T.P. Holme, K. Crabb, W. Lee, Y.B. Kim, X. Tian, T.M. Gür, F.B. Prinz, Enhanced oxygen exchange and incorporation at surface grain boundaries on an oxide ion conductor, *Acta Mater.* 60 (2012) 1–7, <https://doi.org/10.1016/j.actamat.2011.09.050>.
- [16] Y.B. Kim, J.H. Shim, T.M. Gür, F.B. Prinz, Epitaxial and polycrystalline gadolinia-doped ceria cathode interlayers for low temperature solid oxide fuel cells, *J. Electrochem. Soc.* 158 (2011) B1453, <https://doi.org/10.1149/2.001112jes>.
- [17] W.-H. Kim, M.-K. Kim, W.J. Maeng, J. Gatineau, V. Pallem, C. Dussarrat, A. Noori, D. Thompson, S. Chu, H. Kim, Growth characteristics and film properties of cerium dioxide prepared by plasma-enhanced atomic layer deposition, *J. Electrochem. Soc.* 158 (2011) G169, <https://doi.org/10.1149/1.3594766>.
- [18] A. Pfau, K.-D. Schierbaum, The electronic structure of stoichiometric and reduced CeO<sub>2</sub> surfaces: an XPS, UPS and HREELS study, *Surf. Sci.* 6028 (1994), [https://doi.org/10.1016/0039-6028\(94\)90027-2](https://doi.org/10.1016/0039-6028(94)90027-2).
- [19] W.T. Wallace, B.K. Min, D.W. Goodman, The stabilization of supported gold clusters by surface defects, *J. Mol. Catal. A Chem.* 228 (2005) 3–10, <https://doi.org/10.1016/j.molcata.2004.09.085>.
- [20] Y. Nagai, T. Hirabayashi, K. Dohmae, N. Takagi, T. Minami, H. Shinjoh, S. Matsumoto, Sintering inhibition mechanism of platinum supported on ceria-based oxide and Pt-oxide-support interaction, *J. Catal.* 242 (2006) 103–109, <https://doi.org/10.1016/j.jcat.2006.06.002>.
- [21] H.J. Kim, J.G. Yu, S. Hong, C.H. Park, Y.B. Kim, J. An, Ridge-valley nanostructured samaria-doped ceria interlayer for thermally stable cathode interface in low-temperature solid oxide fuel cell, *Phys. Status Solidi A* 214 (2017) 1–6, <https://doi.org/10.1002/pssa.201700465>.